ACS OMEGA

Open Access

http://pubs.acs.org/journal/acsodf

Article

Study on the Nanoaggregate Formation Mechanism and Antipyretic Effect of Maxing Shigan Decoction

Bingbing Zhao, Yanxu Zhang, Zhengmin Fan, Ziwei Lin, Lihong Wang, Hongteng Li, Haojie Zhen, and Chunli Wu*

Cite This: *ACS Omega* 2024, 9, 19311−19319

Read Online

ACCESS | Metrics & More | Article Recommendations | Supporting Information

ABSTRACT: Traditional Chinese medicine (TCM) formula decoctions easily form nanoaggregates due to self-assembly during the decoction process. However, research on nanoaggregates in TCM is still in its infancy with limited systematic studies. Maxing Shigan Decoction (MXSGT), a TCM formula, has been commonly used for the treatment of fever for thousands of years in China. This study used MXSGT as an example to investigate the antipyretic effects of MXSGT nanoaggregates (MXSGT-NAs) in its decoction, shedding light on the compatibility mechanisms of Chinese medicine. MXSGT-NAs were isolated by using high-speed centrifugation and dialysis techniques. The morphology, particle size distribution, and electrical potential of MXSGT-NAs were characterized. High-performance liquid chromatography (HPLC) was used to detect ephedrine and pseudoephedrine in MXSGT-NAs. The self-assembly mechanism of MXSGT-NAs was investigated by deconstructing the prescription. In pharmacodynamic experiments, a rat fever model was established through the subcutaneous injection of dry yeast to investigate the antipyretic effects of MXSGT-NAs. The results showed the presence of regularly shaped spherical nanoaggregates in MXSGT. It contains carbon, oxygen (O), sulfur (S), sodium, aluminum (Al), calcium (Ca), iron, magnesium, bismuth (Bi), etc. MXSGT-NAs exerted substantial antipyretic effects on febrile rats. Furthermore, we found micrometer-sized particles composed of Ca, O, S, potassium, and Bi in Shi gao decoctions. This study is the first to provide evidence for the self-assembling property of Shi gao, elucidate the scientific connotation of dispensing Shi gao in MXSGT, and provide a novel perspective for the study of TCM decoctions.

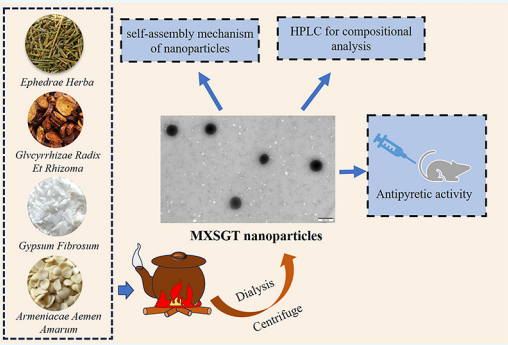

1. INTRODUCTION

In traditional Chinese medicine (TCM), decoctions have long been widely used and are the most frequently employed form of medication.[1] Recently, researchers have discovered the presence of nanoaggregates in TCM decoctions,[2−4] offering a new perspective on the scientific connotation of traditional treatments.[5−7] These nanoparticles have been identified in various decoctions, including Ge-Gen-Qin-Lian-Tang,[8] Huang-Lian-Jie-Du-Tang,[9] and Nao-Luo-Xin-Tong-Tang.[10] Self-assembled submicrometer particles constructed by berberine and curcumin through noncovalent bonding significantly enhance antimicrobial activity.[11] In addition, Ping et al. identified an association between the antipyretic effect of Bai-Hu-Tang and its nanoaggregates.[12] Moreover, Turkish galls were found to contain numerous nanoparticles, exhibiting excellent antimicrobial and antioxidant properties.[13,14] Baicalin and berberine could self-assemble into nanoparticles, which demonstrated better antimicrobial activity than berberine alone.[15] These findings highlight the significance of studying nanoaggregates to understand the material basis of the effects of TCM and emphasize the importance of exploring how nanoaggregates are formed.[16−18] The discovery of self-assembled nanoparticles in TCM decoctions has led researchers to explore the mechanisms underlying their formation.[19−21] Hu et al. analyzed the chemical compositions of both the supernatant and naturally occurring precipitate of Sini decoction and identified that glycyrrhizic acid and three basic compounds (aconitine, hypaconitine, and mesaconitine) undergo a complexation reaction, thereby self-assembling into acid−base complexes.[22] During the decoction process of TCM, various chemical reactions occur, such as hydrolysis, oxidation, and acid−base neutralization.[23] In addition, during the decoction process, ingredients in Chinese medicines are subjected to hydrophobic interactions, van der Waals forces, $\pi-\pi$ stacking, and electrostatic forces, all of which contribute to the self-assembly of components into particulate aggregates.[24,25] In TCM, active ingredients are characterized by

Received: January 12, 2024
Revised: March 7, 2024
Accepted: April 2, 2024
Published: April 16, 2024

Scheme 1. Research Strategy of Isolation, Formation Mechanism, Component Analysis, and Antipyretic Activity of MXSGT-NAs

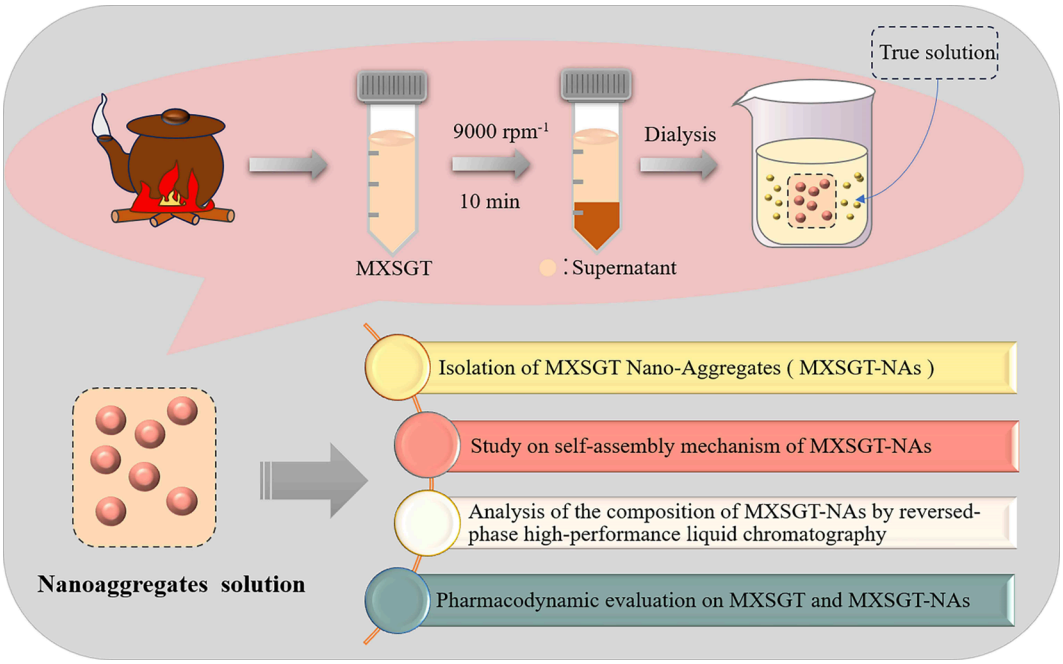

their tendency to self-assemble, including proteins, saccharides, and saponins.[26,27] Furthermore, boiling licorice led to the formation of protein nanoparticles capable of encapsulating astragaloside,[28] thus increasing the solubilization of active components and enhancing the efficacy of the drug.[29] In addition, rhein may self-assemble to form hydrogels through stacking and hydrogen bonding. Furthermore, metal ions dissolved during the decoction process can form nanoparticles with active ingredients through coordination bonding.[30] These spontaneously formed nanoparticles exhibit favorable stability and biocompatibility.[31,32]

Maxing Shigan decoction (MXSGT), a TCM formula first documented in Shang Han Lun, which was compiled by Zhong Jing Zhang over 2000 years ago, has been widely used to treat various diseases such as cough, fever, and pneumonia.[33] It consists of Gypsum Fibrosum (Shi gao), *Ephedrae herba* (Ma huang), Armeniacae Semen Amarum (Ku xing ren), and Glycyrrhizae Radix Et Rhizoma (Gan cao). However, despite its well-known heat-removing and detoxifying properties, the mechanism underlying the antipyretic effect of MXSGT is yet to be fully understood. Ephedrine and pseudoephedrine, key components in MXSGT, exhibit pharmacological activities that are highly correlated with therapeutic functions. Thus, it is necessary to analyze their compositions. However, TCM decoctions are complex multiphase systems. Effective constituents in TCM coatings may not solely comprise chemical components. Nanoaggregates may also contribute to their medicinal effects.[34,35] Pi et al. found the presence of supramolecular structures in MXSGT precipitates.[36] The present study analyzed the antipyretic mechanism of MXSGT from the perspective of self-assembled nanoparticles and explored the material basis for its antipyretic property. In this study, we identified nanoparticles in MXSGT, ranging from 400 to 500 nm in size, following dialysis and centrifugation. We used transmission electron microscopy (TEM) to characterize the morphology of MXSGT nanoaggregates (MXSGT-NAs). To investigate the formation mechanism of MXSGT-NAs, we divided MXSGT into 14 solution groups and performed TEM to characterize their morphology. This analysis enabled us to determine the key factors responsible for the formation of the self-assembled nanoparticles. Subsequently, we analyzed the compositions of ephedrine and pseudoephedrine and determined the elemental distributions in MXSGT-NAs. In addition, we established a dry yeast-induced rat fever model to evaluate the antipyretic effect of MXSGT-NAs (Scheme 1.

2. MATERIALS AND METHODS

2.1. Materials. MXSGT formulation consists of 60 g of *Ephedra sinica* Stapf. stem (sundried; Herba Ephedrae, Ma huang), 30 g of *Glycyrrhiza uralensis* Fisch. (root and rhizome; Radix Glycyrrhizae, Gan Cao), 20 g of *Prunus armeniaca* L. var. *ansu* Maxim. (seed, stir-fried; Semen Armeniacae Amarum, Ku xing ren), and 120 g of gypsum (Gypsum Fibrosum, Shi gao, $CaSO_4{\cdot}2H_2O$). We purchased Ma huang (no. 221001) from Hubei Daodi Herb Technology Co. (Hubei, China), Ku xing ren (no. 190901) from Bozhou Zhang Zhongjing Chinese Medicine Drinking Tablets Co. (Bozhou, China), Gan cao (no. 22080102) from Yunnan Kern Pharmaceutical Drinking Tablets Co. (Yunnan, China), and Shi gao (no. 20210901) from Haiwang Baicaotang Pharmaceutical Co. (Hubei, China).

Ephedrine ($C_{10}H_{16}NO{\cdot}HCl$, 100%) and pseudoephedrine ($C_{10}H_{15}NO{\cdot}HCl$, 99.9%) were purchased from the National Institutes for Food and Drug Control (Beijing, China). Dry yeast was procured from Angie's Yeast Co. The blood calcium (Ca) concentration test kit (no. 2306001), tumor necrosis factor-α (TNF-α) kit, and interleukin (IL)-1β kit were obtained from Beijing Solepol Technology Co. (Beijing, China).

2.2. Animals. Specific pathogen-free (SPF) male Sprague–Dawley (SD) rats (weighing 180 ± 20 g) were purchased from Henan Provincial Laboratory Animal Center [Zhengzhou, Henan; license number: SCXK (Yu) 2017-0001]. The rats

https://doi.org/10.1021/acsomega.4c00423
ACS Omega 2024, 9, 19311−19319

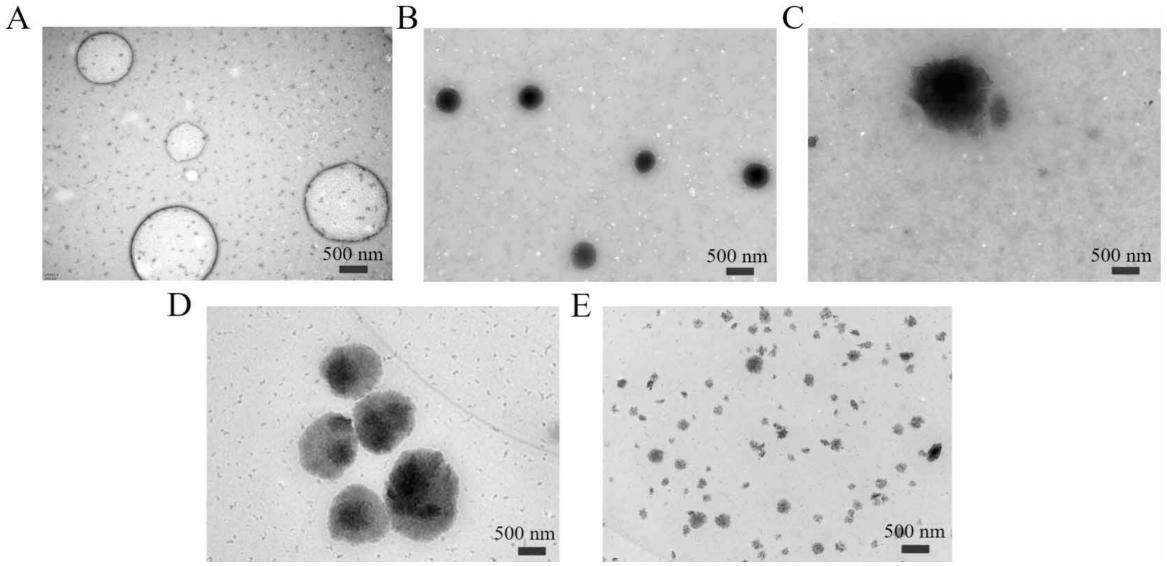

Figure 1. TEM of MXSGT-NAs dialysis in 15 min (A), 30 min (B), 60 min (C), 90 min (D), and 120 min (E).

were housed in SPF-grade animal facilities, individually caged, and provided with ad libitum access to water. The room temperature and relative humidity were maintained at 24 ± 2 °C and 50 ± 10%, respectively. The experiments were conducted in accordance with the Guide for the Care and Use of Laboratory Animals. All animal experiments were approved by the Laboratory Animal Care and Welfare Committee of the Safety Evaluation Centre of Zhengzhou University (ethical clearance number yxyllsc20230067).

2.3. Preparation of MXSGT. According to the renowned publication "Shang Han Lun", authored by Zhongjing Zhang, MXSGT was prepared as follows. First, 60 g of Ma huang was placed into a casserole, and 1400 mL of water was added. This mixture was boiled for 30 min. Subsequently, 120 g of Shi gao, 30 g of Gao Cao, and 20 g of Ku xing ren were added to a casserole and boiled together for 40 min. The resulting mixture was then filtered through four layers of gauze, yielding 600 mL of MXSGT.

2.4. Isolation of MXSGT-NAs. MXSGT was centrifuged at 9000 rpm for 10 min, and 20 mL of the supernatant was transferred to a dialysis bag (15 kDa). The dialysis bag was submerged in a beaker containing 2000 mL of distilled water. The bag was periodically replaced, and the liquid inside of the bag was also collected every 30 min. This process was repeated four times. The four dialysates were dropped on copper grids, and their morphology was observed using TEM after drying.

2.5. Size Distribution, Potential, and Morphological Characterization of MXSGT-NAs. The size distribution and potential of MXSGT-NAs were measured by using a Malvern laser particle sizer (Zetasizer Nano-ZS 90, UK). The morphology of MXSGT-NAs was characterized by using a transmission electron microscope (JEOL JEM-F200, Japan). The elemental distribution of nanoparticles was detected by using energy dispersive X-ray (EDS) elemental mapping during TEM.

2.6. Reversed-Phase High-Performance Liquid Chromatography Analytical Conditions. The samples were separated on a high-performance liquid chromatography (HPLC) system (Waters, MA, USA) equipped with a Phenomenex 00G-4435-E0 C18 column (4.6 × 250 × 5 μm). The mobile phase was composed of 0.1% phosphoric acid in water (A) and acetonitrile (B) with a flow rate of 1 mL/min. The gradient elution program was as follows: (A:B, 2:98) in 30 min. The injection volume, detection wavelength, flow rate, and column temperature were set to 5 μL, 210 nm, and 30 °C, respectively.

Standard ephedrine hydrochloride and pseudoephedrine hydrochloride were weighed appropriately and mixed with methanol to form a control solution. Different volumes (0.5, 0.8, 1, 2, 3, and 5 μL) were injected into the chromatographic system, and standard curves for these different volumes were generated. In addition, 2 mL of MXSGT-NAs was diluted 5-fold with methanol and filtered through a 0.22 μm filter membrane. The peaks of components were identified by comparing the retention times of the samples with those of the standards (ephedrine hydrochloride and pseudoephedrine hydrochloride) in the ultraviolet spectrum.

2.7. Study on the Formation Factors of MXSGT-NAs. The four medicinal materials in the MXSGT decoction were combined into 14 groups as follows: single herb group (Shi gao, Ma huang, Gan cao, and Ku xing ren), two herb groups (Shi gao + Ma huang, Shi gao + Gan cao, Shi gao + Ku xing ren, Gan cao + Ku xing ren, Ma huang + Gan cao, and Ma huang + Ku xing ren), and three herb groups (Ma huang + Shi gao + Gan cao, Ma huang + Gan cao + Ku xing ren, Ma huang + Shi gao + Ku xing ren, and Shi gao + Gan cao + Ku xing ren). For each group, the decoction was prepared by using the same dosage ratios as in the original MXSGT formula. The decoctions were then centrifuged at 9000 rpm for 10 min to remove any precipitate. The resulting supernatant from each group was subjected to dialysis at 37 °C for 30 min using a dialysis bag (15 kDa) to obtain the nanophase solution. Then, the morphologies of the nanophase solutions from all 14 groups were characterized through TEM.

2.8. Pharmacodynamic Evaluation on MXSGT-NAs. Twenty-five male SD rats at 6 weeks of age were selected and fed adaptively for 1 week. The anal temperature was measured for 3 consecutive days, and the rats with anal temperature greater than 38 °C or anal temperature difference greater than 0.5 °C were excluded. They were randomly divided into five groups: blank group, model group, acetaminophen (APAP) group, MXSGT group, and MXSGT-NA group. According to

https://doi.org/10.1021/acsomega.4c00423
ACS Omega 2024, 9, 19311−19319

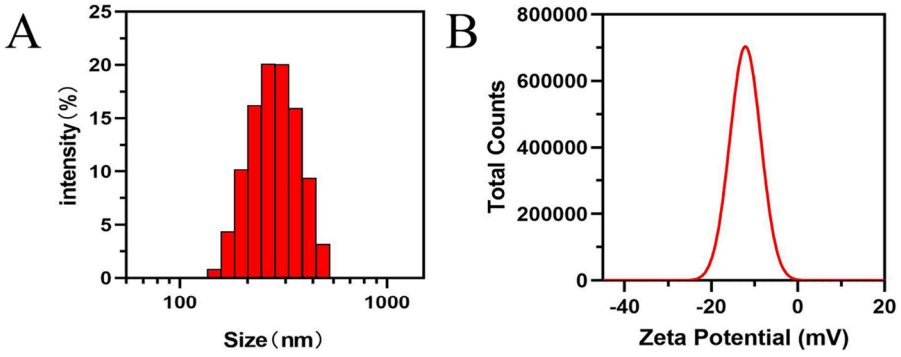

Figure 2. Particle size distribution (A) and zeta potential of MXSGT nanoparticles (B).

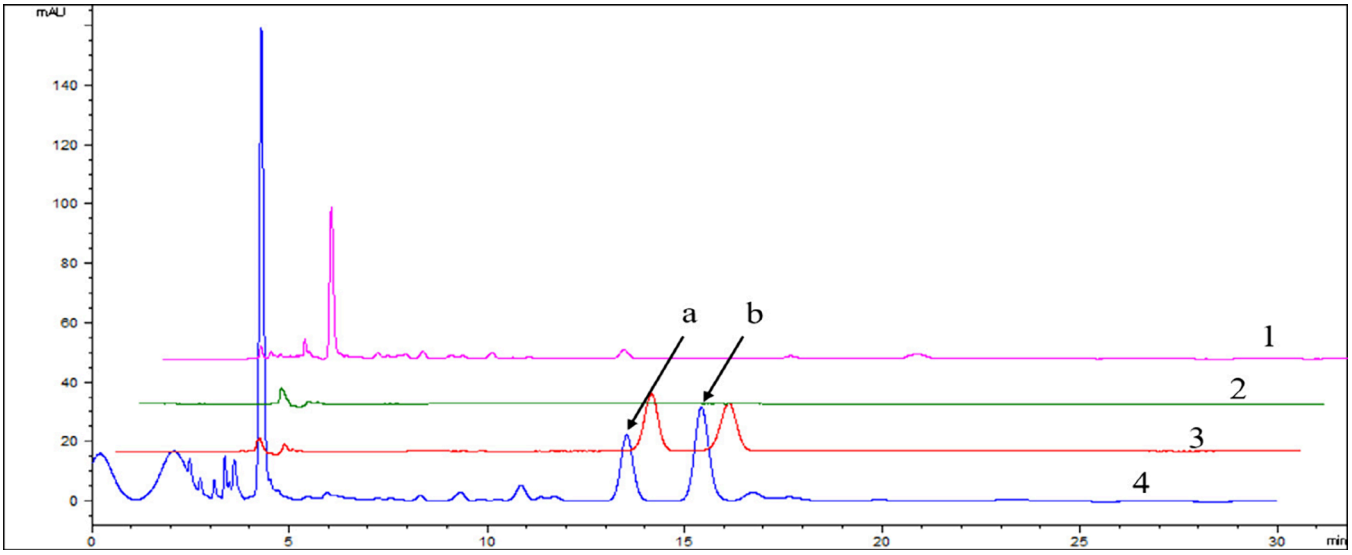

Figure 3. Representative HLPC of MXSGT. (1) MXSGT (no Ma huang), (2) blank baseline, (3) mixture of standard compounds, and (4) MXSGT. (a) Ephedrine hydrochloride. (b) Pseudoephedrine hydrochloride.

previous studies, MXSGT was effective at a dose of 630 mg/kg.[36] Conversion of animal and human equivalent doses based on body surface area discounting yields a dose of 210 mg/kg for APAP. Each administration group was given an intragastric administration. The rats were treated with MXSGT (630 mg/kg) and MXSGT NPs (630 mg/kg) half an hour in advance; the normal and model groups were administered equal volumes of distilled water. Excluding the blank group, 20 rats in the other groups were subcutaneously injected with a 15% dry yeast suspension (10 mL/kg). The anal temperature of the rats was monitored for 10 h after dry yeast injection. Plasma and serum samples were collected, and enzyme-linked immunosorbent assay kits were used to measure the TNF-α and IL-1β levels in serum. In addition, plasma Ca levels were determined.

3. RESULTS AND DISCUSSION

3.1. Morphology, Particle Size Distribution, and Potential of MXST-NAs. We used high-speed centrifugation and dialysis to isolate nanoaggregates from MXSGT. As shown in Figure 1, spherical nanoparticles were successfully obtained through dialysis using a dialysis bag (15 kDa) for 30 min. These nanoparticles exhibited a uniform size distribution ranging from 400 to 500 nm, and they displayed a zeta potential of −11.4 mV (Figure 2). No nanoparticles were obtained at 15 min of dialysis. The morphology of the nanoparticles changed and gradually lost its smooth integrity after 30 min of dialysis. Subsequently, the nanoparticles were observed to be in a fragmented state at 120 min of dialysis. On the basis of these findings, we speculated that the extension of dialysis time altered the morphology of the nanoparticles. Thus, for the separation of nanoparticles in this study, we chose a 30 min dialysis period using a 15 kDa dialysis bag.

3.2. Analysis of Ephedrine and Pseudoephedrine Contents. We analyzed the contents of ephedrine and pseudoephedrine through HPLC (Figure 3). The contents of ephedrine and pseudoephedrine were linearly correlated with the peak area in the range of 10.81−108.01 μg. In particular, the contents of ephedrine and pseudoephedrine were 532.1 and 825.9 μg/mL, respectively, in MXSGT and 138.8 and 326.61 μg/mL, respectively, in MXSGT-NAs. These results indicated the presence of alkaloids in MXSGT-NAs.

3.3. Morphological Characterization of 14 Groups. Figure 4 presents the morphological results of the 14 groups studied. In the Shi gao group, we observed micrometer-sized particles with a regular morphology, measuring 2.5 μm. In the Ma huang group, few agglomerated particles were observed. The Gan cao group revealed spherical nanoparticles with a size of approximately 180 nm along with irregular black aggregates. However, no nanoparticles were observed in the Ku xing ren group.

https://doi.org/10.1021/acsomega.4c00423
ACS Omega 2024, 9, 19311−19319

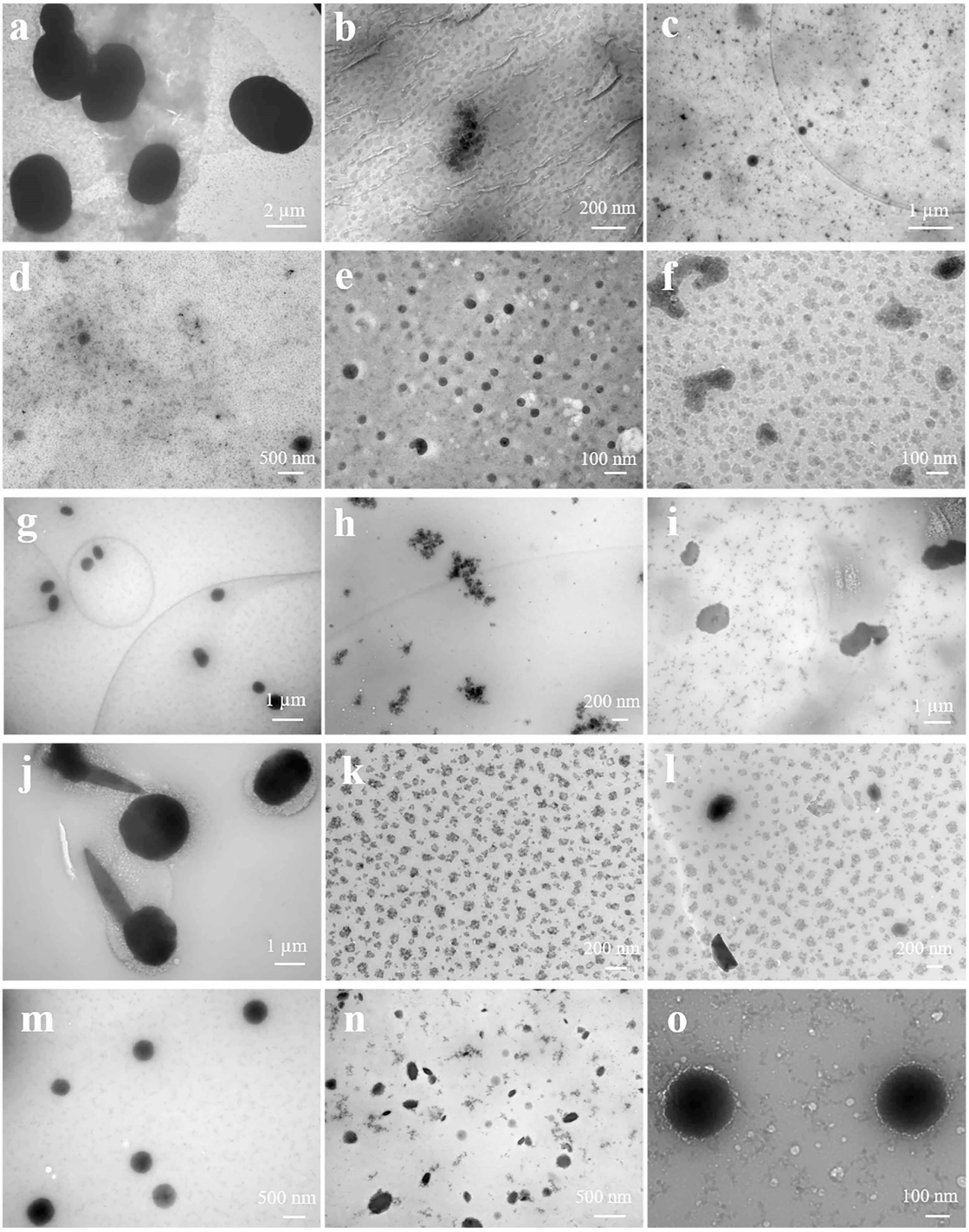

Figure 4. TEM image of 14 groups and MXSGT. (a) Shi gao. (b) Ma huang. (c) Gan cao. (d) Ku xing ren. (e) Ma huang + Gan cao. (f) Ma huang + Ku xing ren. (g) Ma huang + Shi gao. (h) Gan cao + Ku xing ren. (i) Shi gao + Gan cao. (j) Shi gao + Ku xing ren. (k) Ma huang + Gan cao + Ku xing ren. (l) Ma huang + Gan cao + Shi gao. (m) Shi gao + Ma huang + Ku xing ren. (n) Shi gao + Gan cao + Ku xing ren. (o) Ma Huang + Shi gao + Gan cao + Ku xing ren.

When the morphology of the two-herb combinations was analyzed, the Ma huang + Gan cao group exhibited numerous spherical nanoparticles with regular shapes. In the Ma huang + Shi gao group, spherical nanoparticles with particle sizes ranging from 400 to 500 nm were observed. In the Ku xing ren + Shi gao group, nanoparticles with a diameter of approximately 1.5 μm were observed. No nanoparticles were observed in the other groups.

When the morphology of the three-herb combinations was analyzed, the Ma huang + Ku xing ren + Shi gao group exhibited nanoparticles with a size of approximately 500 nm. These nanoparticles had a smooth and rounded surface. The Gao Cao + Shi gao + Ku xing ren group revealed irregular black particles, likely due to the absence of Ma huang, preventing the formation of nanoparticles with a round surface.

3.4. Elemental Analysis Results of Shi Gao and MXSGT-NAs. As shown in Figure 5, the elemental analysis

https://doi.org/10.1021/acsomega.4c00423
ACS Omega 2024, 9, 19311−19319

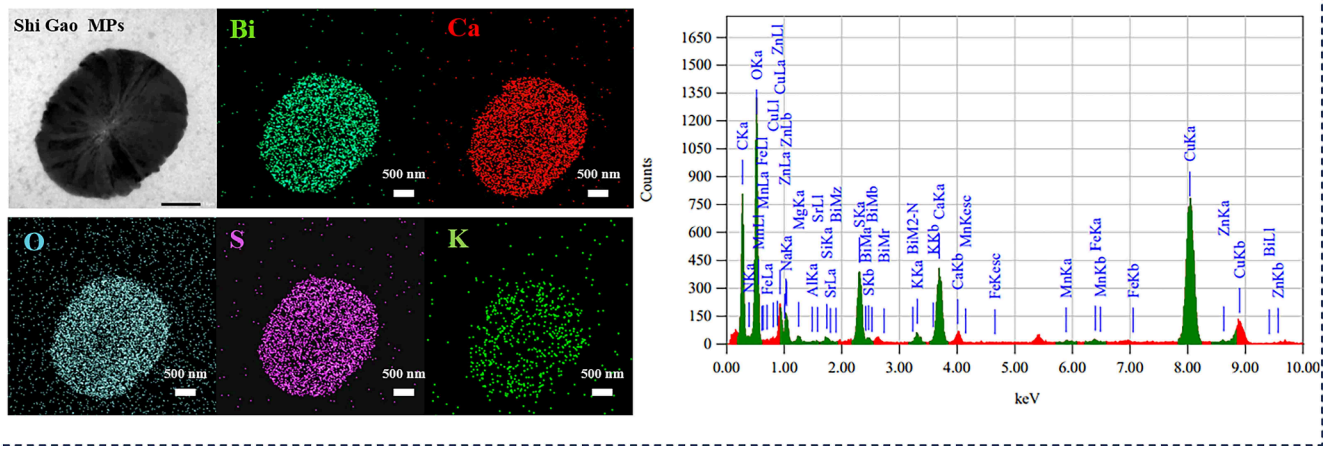

Figure 5. EDS elemental mapping of Shi gao MPs. The results indicated that Shi gao MPs contained C, O, Ca, Mg, K, Bi, Cu, etc.

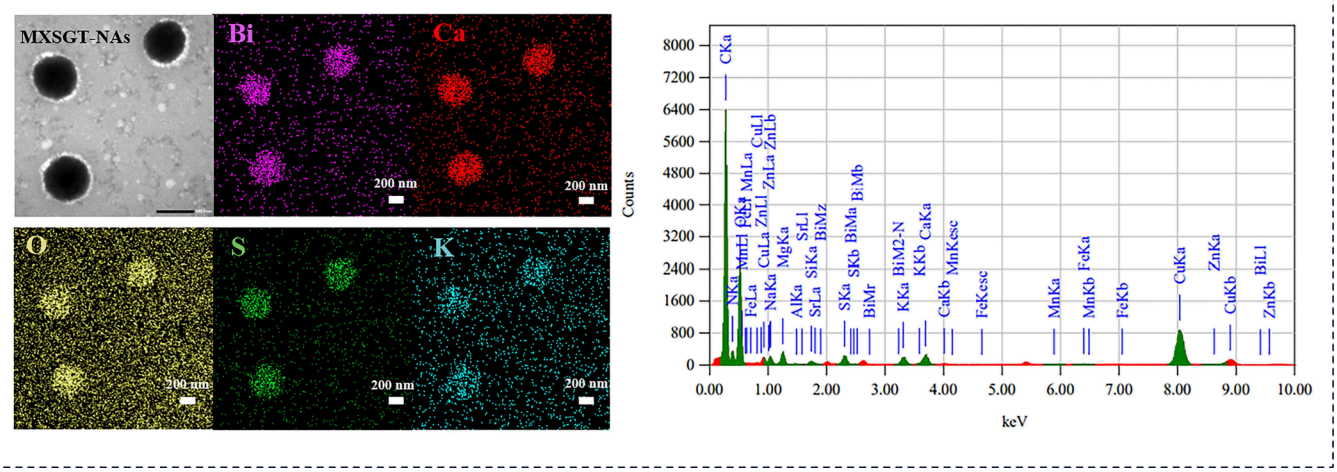

Figure 6. EDS elemental mapping of MXST-NAs. The results indicated that MXST-NAs contained C, O, Ca, Mg, K, Bi, Cu, etc.

indicated that the micrometer-sized particles of Shi gao (Shi gao MPs) were mainly composed of five elements, calcium (Ca), oxygen (O), bismuth (Bi), potassium (K), and sulfur (S). Other elements, such as carbon (C), copper (Cu), aluminum (Al), silicon (Si), nitrogen (N), zinc (Zn), manganese (Mn), etc., were distributed in the scanning range. Shi gao was composed of calcium sulfate and some trace elements. Therefore, we concluded that Shi gao MPs resulted from the self-assembly of calcium sulfate and trace elements during the boiling of the Shi gao decoction.

As shown in Figure 6, Ca, O, Bi, K, and S were markedly distributed in MXSGT-NAs, and all of these elements were involved in the MXSGT self-assembly process. In addition, C, Cu, Al, Si, N, Zn, and other elements that were distributed in the scanning range contributed to the formation of MXSGT-NAs.

3.5. Antipyretic Activity of MXSGT-NAs. As shown in Figure 7A, after the subcutaneous injection of dry yeast, the temperature of the rats in the model group was significantly increased compared with that of the rats in the normal group ($P < 0.01$), indicating the successful establishment of the fever rat model. Both the MXSGT and MXSGT-NA groups exerted antipyretic effects on the febrile rats compared with the model group. However, as shown in Figure 7B,C, the IL-1β and TNF-α levels in the rats in the MXSGT and MXSGT-NA groups were significantly reduced when compared with those in the model group ($P < 0.01$ and $P < 0.01$, respectively). As illustrated in Figure 7D, compared with the model group, both the MXSGT and MXSGT-NA groups exhibited elevated blood Ca levels. These results indicate that MXSGT-NAs exhibit antipyretic pharmacological activity, which constitutes an important pharmacological component of MXSGT.

4. CONCLUSIONS

In this study, we used high-speed centrifugation and dialysis to separate the nanoparticles in MXSGT. MXSGT-NAs might facilitate the uptake and distribution of alkaloids, potentially leading to their superior biological activities compared with ephedrine. Calcium sulfate, other trace elements, and ingredients found in Shi gao, Ma huang, Gan cao, and Ku xing ren formed a natural nanoaggregate during the decoction process. In addition, calcium sulfate and trace elements present in Shi gao exhibited self-assembling properties, undergoing thermal-induced alterations to form micrometer-sized particles during the boiling process. MXSGT-NAs displayed antipyretic pharmacological activity, demonstrating a close relationship between the efficacy of medicinal decoctions and their nanoaggregates. Mineral medicines have a wide range of medicinal values; however, there are mechanisms by which

https://doi.org/10.1021/acsomega.4c00423
ACS Omega 2024, 9, 19311−19319

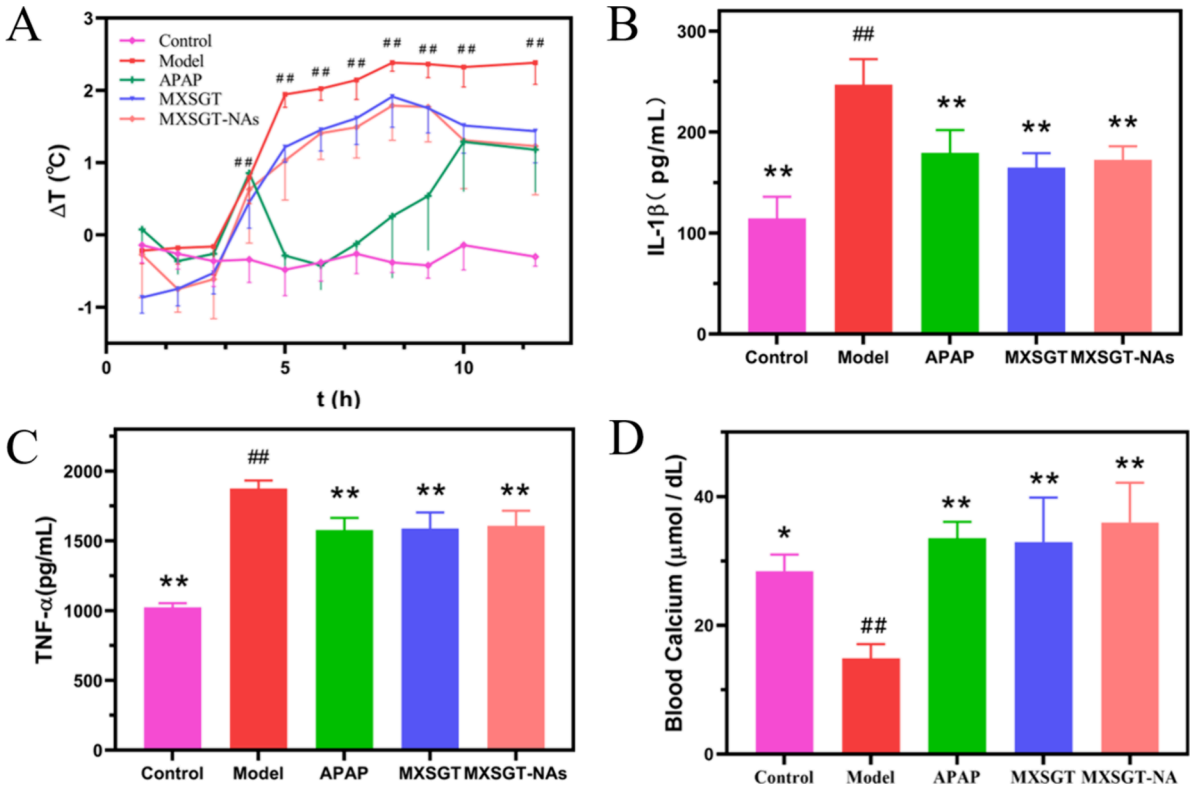

Figure 7. (A) Antipyretic effect of MXSGT and MXSGT-NAs on rats with dry yeast-induced fever. (B, C) Blood was collected 10 h after the injection of dry yeast, and serum TNF-α and IL-1β levels were measured using ELISA kits. (D) Plasma was collected 10 h after the injection of dry yeast, and the plasma Ca content was determined. The model group was compared with the blank group; $^{\#\#}P < 0.05$, $^{\#\#}P < 0.01$ vs the model group; $^{*}P < 0.05$, $^{**}P < 0.01$.

insoluble or essentially insoluble mineral medicines exhibit therapeutic effects in Chinese medicine formulas. In the study, the discovery of gypsum self-assembled particulate structures explained this problem. Trace elements such as insoluble calcium sulfate, Bi, K, and Na in the form of self-assembled particles are present in the decoction. This self-formed particulate structure improved the availability of metallic elements and increased the solubility of insoluble components, thereby demonstrating some biological activity in vivo. The self-assembly phenomenon of Shi gao reveals its scientific connotations in the context of Chinese medicine compounding and provides new perspectives for exploring the material basis of other Shi gao-containing formulations.

■ ASSOCIATED CONTENT

Supporting Information

The Supporting Information is available free of charge at https://pubs.acs.org/doi/10.1021/acsomega.4c00423.

Additional experimental details, materials, and methods (PDF)

■ AUTHOR INFORMATION

Corresponding Author

Chunli Wu − *School of Pharmaceutical Sciences and School of Pharmaceutical Science and Institute of Pharmaceutical Science, Zhengzhou University, Zhengzhou 450001, PR China;* orcid.org/0000-0001-5658-6969; Email: kedi2009@126.com

Authors

Bingbing Zhao − *School of Pharmaceutical Sciences, Zhengzhou University, Zhengzhou 450001, PR China*

Yanxu Zhang − *Henan-Macquarie University Joint Centre for Biomedical Innovation, School of Life Sciences, Henan University, Kaifeng, Henan 475004, China*

Zhengmin Fan − *School of Pharmaceutical Sciences, Zhengzhou University, Zhengzhou 450001, PR China*

Ziwei Lin − *School of Pharmaceutical Sciences, Zhengzhou University, Zhengzhou 450001, PR China*

Lihong Wang − *School of Pharmaceutical Sciences, Zhengzhou University, Zhengzhou 450001, PR China*

Hongteng Li − *School of Pharmaceutical Sciences, Zhengzhou University, Zhengzhou 450001, PR China*

Haojie Zhen − *School of Pharmaceutical Sciences, Zhengzhou University, Zhengzhou 450001, PR China*

Complete contact information is available at: https://pubs.acs.org/10.1021/acsomega.4c00423

Funding

This study did not receive any specific funding from funding agencies in the public, commercial, or nonprofit sectors.

Notes

The authors declare no competing financial interest.

■ ACKNOWLEDGMENTS

This research was supported by Henan-Macquarie University Joint Centre for Biomedical Innovation, School of Life Sciences (Henan University) and School of Pharmaceutical

Science and Institute of Pharmaceutical Science, Zhengzhou University.

■ ABBREVIATIONS

MXSGT: Ma Xing Shi Gan decoction
MXSGT-NA: Ma Xing Shi Gan Tang nanoaggregates
HPLC: high-performance liquid chromatography
APAP: acetaminophen
TCM: traditional Chinese medicine
TEM: transmission electron microscopy
IL-1β: interleukin-1β
TNF-α: tumor necrosis factor-α

■ REFERENCES

(1) Capodice, J. L.; Chubak, B. M. Traditional Chinese herbal medicine-potential therapeutic application for the treatment of COVID-19. *Chin. Med.* **2021**, *16*, 24.
(2) Gao, Y.; Dong, Y.; Guo, Q.; Wang, H.; Feng, M.; Yan, Z.; Bai, D. Study on Supramolecules in Traditional Chinese Medicine Decoction. *Molecules* **2022**, *27*, 3268.
(3) Hou, Y.; Zou, L.; Li, Q.; Chen, M.; Ruan, H.; Sun, Z.; Xu, X.; Yang, J.; Ma, G. Supramolecular assemblies based on natural small molecules: Union would be effective. *Mater. Today Bio* **2022**, *15*, No. 100327.
(4) Jia, X.; Yuan, Z.; Yang, Y.; Huang, X.; Han, N.; Liu, X.; Lin, X.; Ma, T.; Xu, B.; Wang, P.; Lei, H. Multi-functional self-assembly nanoparticles originating from small molecule natural product for oralinsulin delivery through modulating tight junctions. *J. Nanobiotechnol.* **2022**, *20*, 116.
(5) Wei, D.; Yang, H.; Zhang, Y.; Zhang, X.; Wang, J.; Wu, X.; Chang, J. Nano-traditional Chinese medicine: a promising strategy and its recent advances. *J. Mater. Chem. B* **2022**, *10*, 2973−2994.
(6) Tian, X.; Wang, P.; Li, T.; Huang, X.; Guo, W.; Yang, Y.; Yan, M.; Zhang, H.; Cai, D.; Jia, X.; Li, F.; Xu, B.; Ma, T.; Cong, Y.; Lei, H. Self-assembled natural phytochemicals for synergistically antibacterial application from the enlightenment of traditional Chinese medicine combination. *Acta Pharm. Sin. B* **2020**, *10*, 1784−1795.
(7) Ji, H.; Wang, W.; Li, X.; Han, X.; Zhang, X.; Wang, J.; Liu, C.; Huang, L.; Gao, W. Y. Natural small molecules enabled efficient immunotherapy through supramolecular self-assembly in PS3mutated colorectal cancer. *ACS Appl. Mater. Interfaces* **2022**, *14*, 2464−2477.
(8) Lin, D.; Du, Q.; Wang, H.; Gao, G.; Zhou, J.; Ke, L.; Chen, T.; Shao, C.; Rao, P. Antidiabetic Micro-/Nanoaggregates from Ge-Gen-Qin-Lian-Tang Decoction Increase Absorption of Baicalin and Cellular Antioxidant Activity In Vitro. *Biomed Res. Int.* **2017**, *2017*, 1−8.
(9) Wu, J.; Yang, Y.; Yuan, X.; Xu, H.; Chen, Q.; Ren, R.; Zhang, Q.; Hou, Z.; Yin, D. Role of particle aggregates in herbal medicine decoction showing they are not useless: considering Coptis chinensis decoction as an example. *Food Funct.* **2020**, *11*, 10480−10492.
(10) Zhao, G.; Hong, L.; Liu, M.; Jiang, H.; Peng, D.; He, L.; Chen, W. Isolation and Characterization of Natural Nanoparticles in Naoluo Xintong Decoction and Their Brain Protection Research. *Molecules* **2022**, *27*, 1511.
(11) Tian, Y.; Tang, G.; Gao, Y.; Chen, X.; Zhou, Z.; Li, Y.; Li, X.; Wang, H.; Yu, X.; Luo, L.; Cao, Y. Carrier-free small molecular self-assembly based on berberine and curcumin incorporated in submicron particles for improving antimicrobial activity. *ACS Appl. Mater. Interfaces* **2022**, *14*, 10055−10067.
(12) Ping, Y.; Li, Y.; Lü, S.; Sun, Y.; Zhang, W.; Wu, J.; Liu, T.; Li, Y. A study of nanometre aggregates formation mechanism and antipyretic effect in Bai-Hu-Tang, an ancient Chinese herbal decoction. *Biomed. Pharmacother.* **2020**, *124*, No. 109826.
(13) Wang, Z.; Li, W.; Lu, J.; Yuan, Z.; Pi, W.; Zhang, Y.; Lei, H.; Jing, W.; Wang, P. Revealing the active ingredients of the traditional Chinese medicine decoction by the supramolecular strategies and multitechnologies. *J. Ethnopharmacol.* **2023**, *300*, No. 115704.
(14) Huang, J.; Zhu, Y.; Xiao, H.; Liu, J.; Li, S.; Zheng, Q.; Tang, J.; Meng, X. Formation of a traditional Chinese medicine self-assembly nanostrategy and its application in cancer: a promising treatment. *Chin. Med.* **2023**, *18*, 66.
(15) Huang, X.; Wang, P.; Li, T.; Tian, X.; Guo, W.; Xu, B.; Huang, G.; Cai, D.; Zhou, F.; Zhang, H.; Lei, H. Self-Assemblies Based on Traditional Medicine Berberine and Cinnamic Acid for Adhesion-Induced Inhibition Multidrug-Resistant Staphylococcus aureus. *ACS Appl. Mater. Interfaces* **2020**, *12*, 227−237.
(16) Zhu, j.; Zhang, Z.; Wang, R.; Huang, X.; Zhou, Y.; Zhang, K.; Zhong, K.; Gong, L.; Li, L.; Liu, W.; Feng, F.; Qu, W. Nanoparticles derived from Scutellaria barbata and Hedytois diffusa herb pair and their anti-cancer activity. *Pharmacol. Res.* **2022**, *2*, No. 100048.
(17) Liu, Y.; Zhao, L.; Shen, G.; Chang, R.; Zhang, Y.; Yan, X. Coordination self-assembly of natural flavonoids into robust nanoparticles for enhanced in vitro chemo and photothermal cancer therapy. *Colloids Surf., A* **2020**, *598*, No. 124805.
(18) Wang, J.; Zhao, H.; Qiao, w.; Cheng, J.; Han, Y.; Yang, X. Nanomedicine-cum-Carrier by co-assembly of natural small products for synergistic enhanced antitumor with tissues protective actions. *ACS Appl. Mater. Interfaces* **2020**, *12*, 42537−42550.
(19) Zhang, J.; Hu, K.; Di, L.; Wang, P.; Liu, Z.; Zhang, J.; Yue, P.; Song, W.; Zhang, J.; Chen, T.; Wang, Z.; Zhang, Y.; Wang, X.; Zhan, C.; Cheng, Y.; Li, X.; Li, Q.; Fan, J.; Shen, Y.; Han, J.; Qiao, H. Traditional herbal medicine and nanomedicine: converging disciplines to improve therapeutic efficacy and human health. *Adv. Drug Delivery Rev.* **2021**, *178*, No. 113964.
(20) Huang, X.; Liu, X.; Lin, X.; Yuan, Z.; Zhang, Y.; Wang, Z.; Pi, W.; Zhao, H.; Lei, H.; Wang, P. Thermodynamics driving phytochemical self-assembly morphological change and efficacy enhancement originated from single and co-decoction of traditional chinese medicine. *J. Nanobiotechnol.* **2022**, *20*, 527.
(21) Lin, X.; Huang, X.; Tian, X.; Yuan, Z.; Lu, J.; Nie, X.; Wang, P.; Lei, H.; Wang, P. Natural Small-Molecule-Based Carrier-Free Self-Assembly Library Originated from Traditional Chinese Herbal Medicine. *ACS Omega* **2022**, *7*, 43510−43521.
(22) Hu, Q.; Chen, M.; Yan, M.; Wang, P.; Lei, H.; Xue, H.; Ma, Q. Comprehensive analysis of Sini decoction and investigation of acid-base self-assembled complexes using cold spray ionization mass spectrometry. *Microchem. J.* **2022**, *173*, No. 107008.
(23) Zhao, Q.; Luan, X.; Zheng, M.; Tian, X.-H.; Zhao, J.; Zhang, W.-D.; Ma, B.-L. Synergistic Mechanisms of Constituents in Herbal Extracts during Intestinal Absorption: Focus on Natural Occurring Nanoparticles. *Pharmaceutics* **2020**, *12*, 28.
(24) Fan, J.; Yu, H.; Lu, X.; Xue, R.; Guan, J.; Xu, Y.; Qi, Y.; He, L.; Yu, W.; Abay, S.; Li, Z.; Huo, S.; Li, L.; Lv, M.; Li, W.; Chen, W.; Han, B. Overlooked Spherical Nanoparticles Exist in Plant Extracts: From Mechanism to Therapeutic Applications. *ACS Appl. Mater. Interfaces* **2023**, *15*, 8854−8871.
(25) Zheng, J.; Fan, R.; Wu, H.; Yao, H.; Yan, Y.; Liu, J.; Ran, L.; Sun, Z.; Yi, L.; Dang, L.; Gan, P.; Zheng, P.; Yang, T.; Zhang, Y.; Tang, T.; Wang, Y. Directed self-assembly of herbal small molecules into sustained release hydrogels for treating neural inflammation. *Nat. Commun.* **2019**, *10*, 1604.
(26) Gao, G.; He, C.; Wang, H.; Guo, J.; Ke, L.; Zhou, J.; Chong, P.; Rao, P. Polysaccharide nanoparticles from lsatis indigotica Fort. Root decoction: diverstity, cytotoxicity, and antiviral activity. *Nanomaterials* **2022**, *12*, 30.
(27) Qiao, L.; Han, M.; Gao, S.; Shao, X.; Wang, X.; Sun, L.; Fu, X.; Wei, Q. Research progress on nanotechnology for delivery of active ingredients from traditional Chinese medicines. *J. Mater. Chem. B* **2020**, *8*, 6333−6351.
(28) Zhou, J.; Zhang, J.; Gao, G.; Wang, H.; He, X.; Chen, T.; Ke, L.; Rao, P.; Wang, Q. Boiling Licorice Produces Self-Assembled Protein Nanoparticles: A Novel Source of Bioactive Nanomaterials. *J. Agric. Food Chem.* **2019**, *67*, 9354−9361.
(29) Ke, L.-j.; Gao, G.-z.; Shen, Y.; Zhou, J.-w.; Rao, P.-f. Encapsulation of Aconitine in Self-Assembled Licorice Protein

https://doi.org/10.1021/acsomega.4c00423
ACS Omega 2024, 9, 19311−19319

Nanoparticles Reduces the Toxicity In Vivo. *Nanoscale Res. Lett.* **2015**, *10*, 49.
(30) Zheng, R.; Fan, H.; Wu, H.; Yao, Y.; Yan, J.; Liu, L.; Ran, Z.; Sun, L.; Yi, L.; Dang, P.; Gan, P.; Zheng, T.; Yang, Y.; Zhang, T.; Tang, Y.; Wang. Directed self-assembly of herbal small molecules into sustained release hydrogels for treating neural inflammation. *Nat. Commun.* **2019**, *10*, 1604.
(31) Yu, Z.; Gao, G.; Wang, H.; Ke, L.; Zhou, J.; Rao, P.; Chen, T.; Peng, Z.; Zou, J.; Luo, S. Identification of protein-polysaccharide nanoparticles carrying hepatoprotective bioactives in freshwater clam (Corbicula fluminea Muller) soup. *Int. J. Biol. Macromol.* **2020**, *151*, 781−786.
(32) Zheng, K.; Xiong, Y.; Li, Z.; Peng, L.; Guo, Q.; Li, X.; Deng, X. ESI-TOF MS analysis and DNA cleavage activity of complexes formed by luteolin and five metal ions in hot water. *Inorg. Nano-Met. Chem.* **2020**, *50*, 1181−1188.
(33) Guo, T.; Guo, Y.; Liu, Q.; Xu, Y.; Wei, L.; Wang, Z.; Chen, S.; Wang, C.; Tian, Y.; Cui, J.; Wang, Y.; Wang, Y.; Sun, L. The TCM prescription Ma-xing-shi-gan-tang inhibits Streptococcus pneumoniae pathogenesis by targeting pneumolysin. *J. Ethnopharmacol.* **2021**, *275*, No. 114133.
(34) Li, T.; Wang, P.; Guo, W.; Huang, X.; Tian, X.; Wu, G.; Xu, B.; Li, F.; Yan, C.; Liang, X.; Lei, H. Natural Berberine-Based Chinese Herb Medicine Assembled Nanostructures with Modified Antibacterial Application. *ACS Nano* **2019**, *13*, 6770−6781.
(35) Iravani, S.; Varma, R. Plant-Derived Edible Nanoparticles and miRNAs: Emerging Frontier for Therapeutics and Targeted Drug-Delivery. *ACS Sustain. Chem. Eng.* **2019**, *7*, 8055−8069.
(36) Pi, W.; Han, N.; Wu, L.; Zhang, X.; Huang, X.; Wang, Z.; Yuan, Z.; Wang, P. Discovery, traceability, formation mechanism, metal and organic components analysis of supramolecules from Maxing Shigan decoction. *J. Pharm. Biomed. Anal.* **2023**, *234*, No. 115532.

https://doi.org/10.1021/acsomega.4c00423
ACS Omega 2024, 9, 19311−19319